Neoplasma 2020; 67(6): 1256–1265

doi:10.4149/neo_2020_191119N1187

Long noncoding RNA UCA1 regulates CCR7 expression to promote tongue squamous cell carcinoma progression by sponging miR-138-5p

T. T. SHI, R. LI, L. ZHAO*

Department of Stomatology, Binzhou People's Hospital, Binzhou, Shandong, China

**Correspondence: fvwyij@163.com*

Received November 19, 2019 / Accepted March 4, 2020

Tongue squamous cell carcinoma (TSCC) is a malignant tumor. Long noncoding RNAs (lncRNAs) have been proved to be involved in the regulation of the progression of various cancers. However, the mechanism of lncRNA urothelial cancer-associated 1 (UCA1) in the progression of TSCC remains unclear. The expression levels of UCA1, microRNA-138-5p (miR-138-5p), and CC chemokine receptor 7 (CCR7) were measured by quantitative real-time polymerase chain reaction (qRT-PCR). The proliferation, migration, and invasion were detected using colony formation assay and transwell assay, respectively. Western blot (WB) analysis was used to test the levels of proliferation and metastasis-related proteins and CCR7 protein. Moreover, the extracellular acidification rate (ECAR) of cells was measured by the Seahorse XF Extracellular Flux Analyzer, and the adenosine triphosphate (ATP) level, glucose uptake, and lactate produce of cells were tested by their corresponding assay kits. Further, the dual-luciferase reporter assay was used to confirm the interaction between miR-138-5p and UCA1 or CCR7. In addition, the effect of UCA1 on TSCC tumor growth *in vivo* was evaluated by animal experiments. We found that UCA1 and CCR7 were upregulated, while miR-138-5p was downregulated in TSCC tissues. Silenced UCA1 restrained the proliferation, migration, invasion, and glycolysis metabolism of TSCC cells. Similarly, knockdown of CCR7 also could suppress the progression of TSCC. Besides, UCA1 overexpression promoted TSCC progression, while this promotion effect could be reversed by CCR7 silencing. miR-138-5p could be sponged by UCA1 and could target CCR7. Additionally, miR-138-5p overexpression could reverse the promotion effect of overexpressed UCA1 on TSCC progression. Furthermore, the UCA1 knockdown reduced TSCC tumor growth *in vivo*. In conclusion, lncRNA UCA1 might function as an oncogene in TSCC through regulating the miR-138-5p/CCR7 axis, providing a new biomarker for TSCC treatment.

Key words: tongue squamous cell carcinoma (TSCC), UCA1, CCR7, miR-138-5p

Tongue squamous cell carcinoma (TSCC) is a common type of oral cancer, accounting for about 25–40% of oral cancers [1]. Although the clinical treatment of TSCC has made great progress, the 5-year survival rate is still less than 50% [2]. Most patients with advanced TSCC have local infiltration or even lymph node metastasis, and often occur postoperative recurrence [3, 4]. Therefore, exploring new biomarkers is of great clinical significance for early diagnosis of TSCC.

Long non-coding RNAs (lncRNAs) are a class of functional RNA molecules that have been studied more in recent years [5]. Studies have demonstrated that lncRNAs are often expressed abnormally in many diseases, including cancer [6, 7]. Many lncRNAs have also been associated with the development of TSCC, such as CACS15, FALEC, and THOR [8–10]. Urothelial cancer associated 1 (UCA1) is a lncRNA derived from bladder cancer [11]. In recent years, lncRNA UCA1 has been found to be widely expressed in other cancers and has been confirmed to have strong carcinogenic activity [12, 13]. Fang et al. reported that UCA1 was upregulated in TSCC and correlated with the metastasis of TSCC [14]. However, the mechanism of UCA1 in TSCC progression is still not clear.

CC chemokine receptor 7 (CCR7) is a member of the G-protein coupled heptad-helix receptor (GPCR) family [15]. Studies had shown that CCR7 expression was related to the invasion and migration of many cancers, including breast cancer and bladder cancer [16, 17]. Not only that, CCR7 had also been linked to the prognosis of cancer patients [18]. More importantly, the results of Feng et al. indicated that CCR7 had a high expression in TSCC [19]. Nevertheless, the exploration of CCR7 might help us better understand the mechanism of cancer metastasis.

At present, studies had proved that lncRNAs could play a regulatory role through a variety of mechanisms, among which they functioned as the sponges of microRNAs

(miRNAs) had been proved most [20]. The purpose of this study was to investigate the function of UCA1 in TSCC progression and reveal the regulation network of its acting as the competitive endogenous RNA (ceRNA), so as to provide a reliable biomarker for TSCC treatment.

Patients and methods

Samples collection. TSCC tissues and the adjacent normal tissues were obtained from 37 TSCC patients who recruited from Binzhou People's Hospital. All patients had written informed consent, and their clinicopathological characteristics were shown in Table 1. All study protocols were approved by the Ethics Committee of Binzhou People's Hospital.

Cell culture. TSCC cell lines (SCC4, SCC15, SCC25, and CAL-27) were bought from the American Type Culture Collection (ATCC, Manassas, VA, USA). Besides, TSCC cell line (UM2, UM1) and human normal squamous epithelial cells (NOK-SI) were obtained from Guandao Bio (Shanghai, China). All cells were cultured in Dulbecco's modified Eagle's medium (DMEM; Gibco, Carlsbad, CA, USA) containing 10% fetal bovine serum (FBS; Gibco), 100 U/ml penicillin and 100 μg/ml streptomycin (Solarbio, Beijing, China) at 37 °C in 5% CO_2 incubator.

Quantitative real-time polymerase chain reaction (qRT-PCR). Total RNAs were extracted using Trizol reagent (Invitrogen, Carlsbad, CA, USA) and reverse-transcribed into complementary DNA (cDNA) using the PrimeScript RT reagent Kit with gDNA Eraser (Takara, Dalian, China). qRT-PCR was performed using SYBR Green (Takara). Relative expression was determined using the $2^{-\Delta\Delta Ct}$ method and normalized using glyceraldehyde 3-phosphate dehydrogenase (GAPDH) or U6. The primers were listed as follows: UCA1, F 5'-CATGCTTGACACTTGGTGCC-3', R 5'-GGTCGCAGGTGGATCTCTTC-3'; CCR7, F 5'-CTGGTGGTGGCTCTCCTTGT-3', R 5'-TCGTCCGTGACCTCATCTTG-3'; GAPDH, F 5'-GACTCATGACCACAGTCCATGC-3', R 5'-AGAGGCAGGGATGATGTTCTG-3'; miR-138-5p, F 5'-GCGAGCTGGTGTTGTGAATC-3', R 5'-AGTGCAGGGTCCGAGGTATT-3'; U6, F 5'-CTCGCTTCGGCAGCACA-3', R 5'-AACGCTTCACGAATTTGCGT-3'.

Western blot (WB) analysis Tissues and cells were lysed using RIPA buffer (Beyotime, Shanghai, China), and lysates were collected. Equal amounts of protein were separated by sodium dodecyl sulfate-polyacrylamide gel electrophoresis (SDS-PAGE) gel and transferred onto polyvinylidene fluoride (PVDF) membranes (Millipore, Billerica, MA, USA). After blocked with 5% skim milk, the membranes were incubated with primary antibodies against CCR7 (1:5000, ab32527, Abcam, Cambridge, MA, USA), c-myc (1:1000, ab32072, Abcam), proliferating cell nuclear antigen (PCNA; 1:1000, bs-0754R, Bioss, Beijing, China), Ki-67 (1:200, bs-23102R, Bioss), matrix metalloproteinase 2 (MMP2, 1:1000, bs-20705R, Bioss), MMP9 (1:500, bs-4593R, Bioss), E-cadherin (1:50, ab40772, Abcam), Vimentin (1:500, ab92547, Abcam) or GAPDH (1:1000, ab9485, Abcam) at 4 °C overnight. Then, the membranes were incubated with secondary antibody (1:2000, ab205718, Abcam) for 1 h, and the protein signals were revealed with enhanced chemiluminescence (GE Healthcare, Shanghai, China).

Cell transfection. UCA1 small interfering RNA (siRNA), lentiviral short hairpin RNA (shRNA) and overexpression plasmid (si-UCA1, sh-UCA1, and UCA1) or their negative controls (si-NC, sh-NC and vector), CCR7 siRNA (si-CCR7) and its negative control (si-NC), miR-138-5p mimic and inhibitor (miR-138-5p and anti-miR-138-5p) or their negative controls (miR-NC and anti-NC) were synthesized by Ribobio (Guangzhou, China). Lipofectamine 3000 (Invitrogen) was used to transfect all plasmid vectors into CAL-27 and UM1 cells.

Cell proliferation assay. The proliferation ability of cells was detected by colony formation assay. Briefly, CAL-27 and UM1 cells were seeded into 6-well plates. After transfection, cells were incubated for 14 d. After that, CAL-27 and UM1 cells were fixed and stained, and the number of cloned cells (>50 cells) was counted.

Transwell assay. Cell migration and invasion abilities were measured by transwell assay. All the assays were performed in transwell chambers (Corning Inc., Corning, NY, USA), in which the invasion assay was executed in the upper chambers coated with a Matrigel (Corning Inc.), while the migration assay in non-coated. Briefly, CAL-27 and UM1 cells were seeded into the upper chambers with serum-free medium, and the lower chambers contained serum medium. After 24 h, cells were fixed and stained, and the number of migrated and invaded cells was counted.

Table 1. Clinicopathological characteristics of TSCC patients.

Clinical parameter	(n=37)
Age (years)	
<60	24
>60	13
Gender	
Male	22
Female	15
Histological grade	
Low or undiffer	14
Middle or high	23
TNM stages	
I and II	25
III and IV	12
Lymphatic metastasis	
Yes	27
No	10
Distant metastasis	
Yes	20
No	17

Detection of extracellular acidification rate (ECAR). After transfection for 48 h, glucose, oligomycin (OM), and 2-deoxy glucose (2-DG) (Seahorse Bioscience, Billerica, MA, USA) were added to CAL-27 and UM1 cells at the indicated points. The ECAR of cells was monitored by the Seahorse XF Extracellular Flux Analyzer (Seahorse Bioscience).

Measurement of adenosine triphosphate (ATP), glucose, and lactate. According to the manufacturer's agreement, the ATP level, glucose uptake, and lactate production of cells were measured by ATP Assay Kit, Glucose Assay Kit, and Lactate Assay Kit (Amyjet, Wuhan, China) after transfection for 48 h, respectively.

Animal experiments. BALB/c nude mice (male) were bought from the Beijing HFK Bioscience Co., Ltd. (Beijing, China). CAL-27 cells transfected with sh-UCA1 or sh-NC were subcutaneously injected into nude mice. Tumor length and width were measured once every 7 d. After 28 d, the tumors were collected and stored at −80 °C until use. All animal experiments were approved by the Ethics Committee of Binzhou People's Hospital.

Dual-luciferase reporter assay. The sequences of UCA1 and CCR7 3'UTR containing the miR-138-5p binding sites and mutant binding sites were inserted into the pmirGLO reporter vectors (Enzyme Research, Shanghai, China) to construct WT/MUT-UCA1 and WT/MUT-CCR7 3'UTR vectors, respectively. CAL-27 and UM1 cells were seeded into 24-well plates and cultured for 24 h. Then, Lipofectamine 3000 (Invitrogen) was used to co-transfect the reporter vectors and miR-138-5p mimic or miR-NC into CAL-27 and UM1 cells. After 48 h, Dual-Luciferase Reporter Assay Kit (Beyotime) was used to assess the luciferase activity of cells.

Statistical analysis. All data were analyzed by GraphPad Prism 5.0 software (GraphPad Software, San Diego, CA, USA) and represented as mean ± standard deviation (SD). Student's t-test or one-way analysis of variance was used for statistical analysis. A p-value <0.05 was defined as statistically significant.

Results

UCA1 was related to miR-138-5p and CCR7 in TSCC. Firstly, we tested the expression of UCA1 and CCR7 in TSCC tissues. As presented in Table 2, we found that UCA1 and CCR7 were remarkably overexpressed in TSCC tissues compared with that in adjacent normal tissues. Interestingly, we uncovered that miR-138-5p was significantly lower expressed in TSCC tissues. Additionally, correlation analysis revealed that miR-138-5p was negatively correlated with UCA1 expression, while CCR7 was positively correlated with UCA1 expression in TSCC tissues (Figures 1A, 1B). To further explore the level of UCA1 in TSCC, we also detected UCA1 expression in TSCC cell lines. Compared to NOK-SI cells, UCA1 expression was markedly promoted in the TSCC cell lines (UM2, UM1, SCC4, SCC15, SCC25, and CAL-27) (Figure 1C). Therefore, we concluded that UCA1 might play an important role in TSCC and might be related to miR-138-5p and CCR7 expression.

Silencing of UCA1 inhibited the proliferation, migration, invasion, and glycolysis of TSCC cells. To investigate the role of UCA1 in TSCC, we used si-UCA1 to knock down its expression in CAL-27 cells. qRT-PCR results revealed that si-UCA1 could effectively inhibit UCA1 expression, indicating a good transfection efficiency (Figure 2A). Thus, we explored the effect of UCA1 silencing on the proliferation, migration, invasion, and glycolysis of CAL-27 cells. Colony formation assay results indicated that the number of cloned CAL-27 cells was obviously decreased in the si-UCA1 group compared with the si-NC group (Figure 2B). Also, we detected

Table 2. Relative expression in TSCC tissues (TSCC) and adjacent normal tissues (ANT).

RNA	ANT (n=37)	TSCC (n=37)	p-value
UCA1	1.04±0.36	2.48±0.66	<0.0001
miR-138-5p	1.00±0.30	0.45±0.21	<0.0001
CCR7	0.99±0.39	2.90±0.58	<0.0001

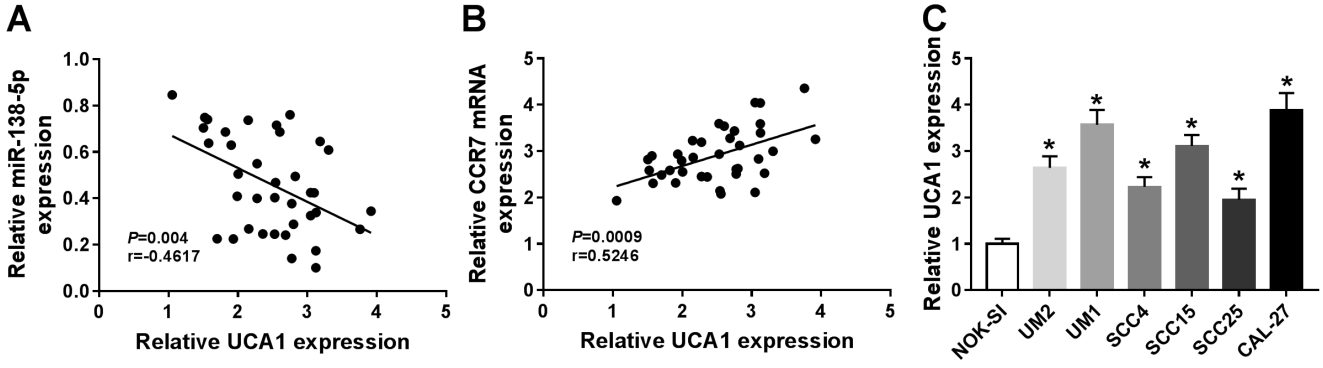

Figure 1. UCA1 was related to miR-138-5p and CCR7 in TSCC. A, B) The correlation between UCA1 and miR-138-5p or CCR7 was measured by Pearson correlation analysis. C) qRT-PCR was used to determine the expression of UCA1 in TSCC cell lines (UM2, UM1, SCC4, SCC15, SCC25, and CAL-27) and NOK-SI cells. *p<0.05

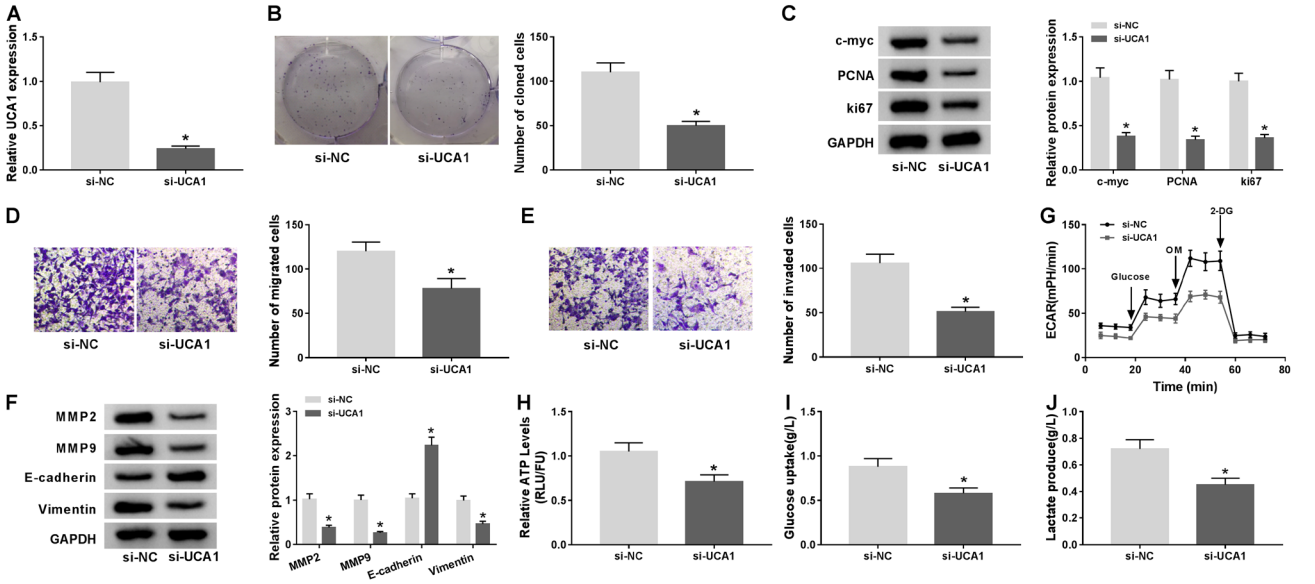

Figure 2. Effect of UCA1 silencing on the progression of CAL-27 cells. CAL-27 cells were transfected with si-UCA1 or si-NC. A) The expression of UCA1 was detected by qRT-PCR to evaluate the transfection efficiency of si-UCA1. B) Colony formation assay results showed that the proliferation of CAL-27 cells was inhibited by UCA1 silencing. C) WB analysis revealed that the knockdown of UCA1 restrained the protein levels of c-myc, PCNA, and Ki-67 in CAL-27 cells. D, E) Transwell assay results indicated that the migration and invasion of CAL-27 cells were suppressed by UCA1 knockdown. F) WB analysis was performed to detect the protein levels of MMP2, MMP9, E-cadherin, and Vimentin in CAL-27 cells. G) The ECAR of CAL-27 cells was measured by Seahorse XF Extracellular Flux Analyzer. H–J) Knockdown of UCA1 markedly increased the ATP level, glucose uptake, and lactate production of CAL-27 cells. *p<0.05

the levels of proliferation-related proteins using WB analysis and found that silenced UCA1 suppressed the protein levels of c-myc, PCNA, and Ki-67 in CAL-27 cells (Figure 2C), which once again confirmed that the knockdown of UCA1 significantly reduced the proliferation ability of TSCC cells. Transwell assay results showed that the silencing of UCA1 remarkably hindered the number of migrated CAL-27 cells (Figure 2D). Also, the number of invaded CAL-27 cells was markedly decreased in the si-UCA1 group compared with the si-NC group (Figure 2E). These results suggested that the knockdown of UCA1 suppressed the migration and invasion of TSCC cells. Furthermore, WB analysis was also carried out to detect the expression of metastasis-related proteins, and the results showed that the expression of MMP2, MMP9, and Vimentin was significantly decreased, while E-cadherin protein level was markedly increased in the si-UCA1 group (Figure 2F). Through measuring the ECAR level of CAL-27 cells, we found that the knockdown of UCA1 markedly reduced the ECAR level of CAL-27 cells (Figure 2G). Moreover, the ATP level of CAL-27 cells was remarkably decreased in the si-UCA1 group compared with the si-NC group (Figure 2H). Furthermore, we also discovered that the silencing of UCA1 significantly hindered the glucose uptake and lactate production of CAL-27 cells (Figures 2I, 2J). Similarly, we performed the same test with UM1 cells, and the results were consistent with CAL-27 cells (Supplementary Figure S1). These data revealed that that UCA1 played a vital role in the progression of TSCC.

Silenced CCR7 hindered the proliferation, migration, invasion, and glycolysis of TSCC cells. At the same time, we found that the protein level of CCR7 was also increased in CAL-27 cells (Figure 3A). Therefore, we transfected si-CCR7 into CAL-27 cells to measure the function of CCR7 knockdown on TSCC progression. The decrease of CCR7 expression after si-CCR7 transfection indicated that the transfection efficiency of si-CCR7 was good, and follow-up experiments could be conducted (Figure 3B). Colony formation assay results suggested that silenced CCR7 inhibited the number of cloned CAL-27 cells (Figure 3C), and WB analysis indicated that the protein levels of c-myc, PCNA, and Ki-67 were markedly decreased in the si-CCR7 group, which indicated that CCR7 knockdown restrained the proliferation of TSCC cells (Figure 3D). Furthermore, the number of migrated and invaded CAL-27 cells was obviously hindered in the CCR7 silencing group (Figures 3E, 3F), suggesting that knockdown of CCR7 suppressed the migration and invasion of TSCC cells, as evidenced by decreased the protein levels of MMP2, MMP9, and Vimentin, and increased E-cadherin level in the si-CCR7 group (Figure 3G). In addition, we also discovered that the silencing of CCR7 restrained the ECAR level, ATP level, glucose uptake, and lactate production of CAL-27 cells (Figures 3H–3K), revealing that CCR7 knockdown suppressed the glycolytic metabolism of TSCC cells. Furthermore, we also found similar results in UM1 cells transfected with si-CCR7 (Supplementary Figure S2).

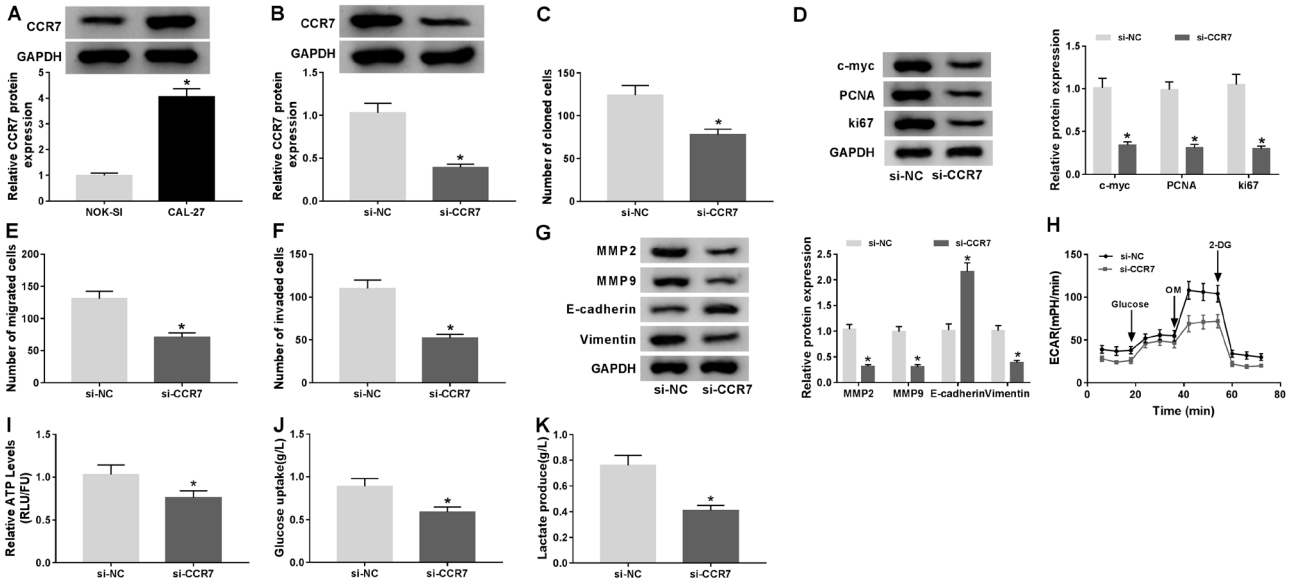

Figure 3. Effect of CCR7 silencing on the progression of CAL-27 cells. A) CCR7 expression was markedly elevated in CAL-27 cells compared to NOK-SI cells. B–K) CAL-27 cells were transfected with si-CCR7 or si-NC. (B) The protein level of CCR7 was detected by WB analysis to evaluate the transfection efficiency of si-CCR7. (C) Colony formation assay results indicated that CCR7 knockdown could repress the proliferation of CAL-27 cells. (D) WB analysis results suggested that CCR7 silencing could hinder the protein levels of c-myc, PCNA, and Ki-67 in CAL-27 cells. (E–F) Transwell assay results showed that the migration and invasion of CAL-27 cells were decreased by CCR7 knockdown. (G) WB analysis was used to determine the protein levels of MMP2, MMP9, E-cadherin, and Vimentin in CAL-27 cells. (H) The ECAR of CAL-27 cells was measured by Seahorse XF Extracellular Flux Analyzer. (I–K) Silenced CCR7 remarkably inhibited the ATP level, glucose uptake, and lactate production of CAL-27 cells. *p<0.05

Therefore, these results confirmed that CCR7 might play a positive role in the progression of TSCC.

Knockdown of CCR7 could reverse the promotion effect of UCA1 overexpression on the progression of CAL-27 cells. Through the above experimental results, we found that the effect of CCR7 knockdown on TSCC cells was similar to that of UCA1 silencing. To verify the effect relationship between CCR7 and UCA1, we transfected with UCA1 overexpression plasmid and si-CCR7 into CAL-27 cells. The increased UCA1 expression showed that the transfection efficiency of UCA1 overexpression plasmid was good (Figure 4A). Through the detection of the proliferation ability of TSCC cells, we found that UCA1 overexpression promoted the number of cloned cells and the protein levels of c-myc, PCNA, and Ki-67 in CAL-27 cells, while CCR7 knockdown could invert this promotion effect (Figures 4B, 4C). Besides, overexpressed UCA1 also increased the number of migrated and invaded CAL-27 cells, accelerated the protein levels of MMP2, MMP9, and Vimentin, and inhibited E-cadherin protein level, but this effect also could be reversed by CCR7 silencing (Figures 4D–4F). Moreover, silenced CCR7 inverted the acceleration effect of UCA1 overexpression on the ECAR level, ATP level, glucose uptake, and lactate production of CAL-27 cells (Figures 4G–4J). At the same time, we also discovered similar results in UM1 cells (Supplementary Figure S3). All data indicated that CCR7 might be a downstream gene of UCA1.

UCA1 regulated CCR7 expression through sponging miR-138-5p. To explore the mechanism of UCA1, we used the miRcode tool to predict the potential target miRNAs of UCA1. And we found that miR-138-5p had complementary sites with UCA1. At the same time, we also discovered that CCR7 3'UTR had binding sites with miR-138-5p using the starBase tool (Figure 5A). Besides, dual-luciferase reporter assay results revealed that the overexpression of miR-138-5p remarkably suppressed the luciferase activity of WT-UCA1 and WT-CCR7 3'UTR vectors, while had no effect on the luciferase activity of MUT-UCA1 and MUT-CCR7 3'UTR vectors in CAL-27 cells (Figures 5B, 5C), which confirmed the interaction between miR-138-5p and UCA1 or CCR7. Also, the expression of miR-138-5p was increased by UCA1 knockdown and decreased by UCA1 overexpression (Figure 5D). To investigate the effect of the miR-138-5p expression on CCR7, we transfected miR-138-5p mimic and inhibitor into CAL-27 cells. qRT-PCR results revealed that miR-138-5p mimic markedly increased miR-138-5p expression in CAL-27 cells, while anti-miR-138-5p could decrease its expression, suggesting that the transfection of both was successful (Figure 5E). Through the detection of the CCR7 protein level, we discovered that the protein level of CCR7 was inhibited by miR-138-5p overexpression, while promoted by miR-138-5p inhibition (Figure 5F). Furthermore, overexpressed UCA1 increased CCR7 protein level, whereas this promotion effect could be reversed by miR-138-5p overexpression, indicating that CCR7 expression was regulated

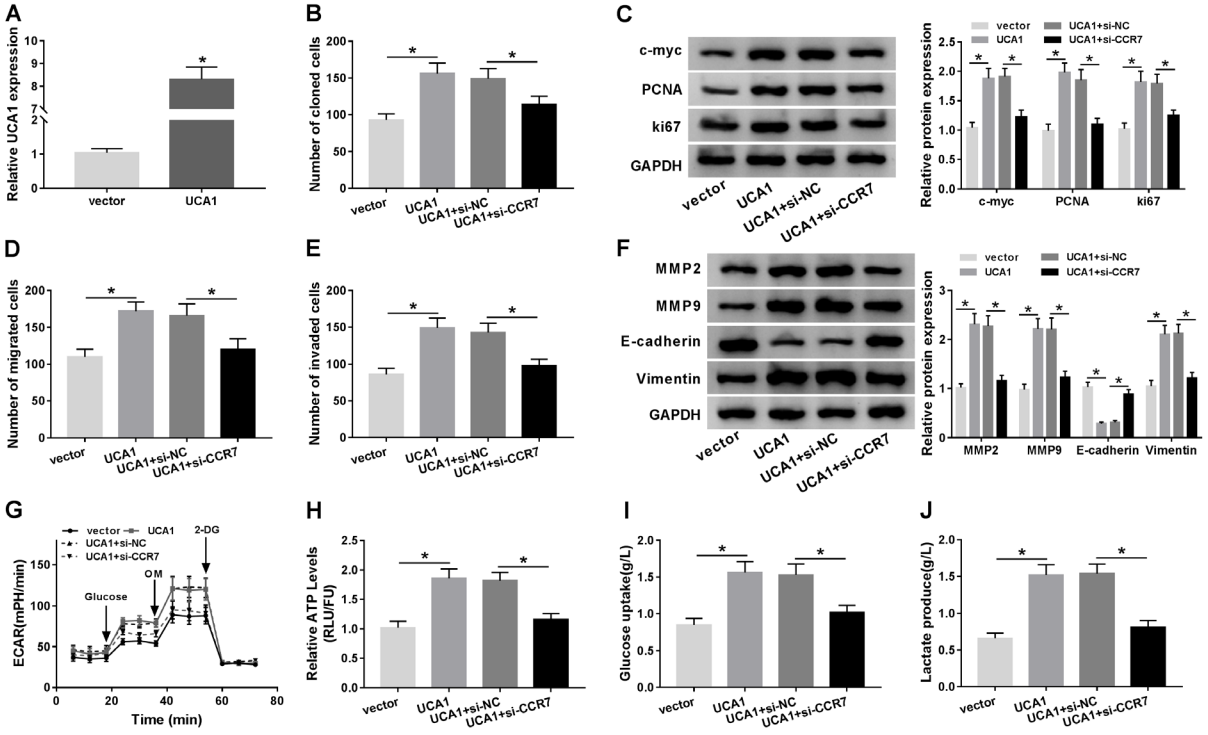

Figure 4. Effects of UCA1 overexpression and CCR7 knockdown on the progression of CAL-27 cells. A) The expression of UCA1 was detected by qRT-PCR to evaluate the transfection efficiency of UCA1 overexpression plasmid. B–J) CAL-27 cells were co-transfected with UCA1 overexpression plasmid and si-CCR7. (B) Colony formation assay was performed to measure the number of cloned CAL-27 cells. (C) WB analysis was used to determine the protein levels of c-myc, PCNA, and Ki-67 in CAL-27 cells. (D–E) The number of migrated and invaded CAL-27 cells was detected by transwell assay. (F) The protein levels of MMP2, MMP9, E-cadherin, and Vimentin in CAL-27 cells were assessed by WB analysis. (G) Seahorse XF Extracellular Flux Analyzer was used to test the ECAR of CAL-27 cells. (H–J) The ATP level, glucose uptake, and lactate production of CAL-27 cells were determined by their corresponding Assay Kits. *p<0.05

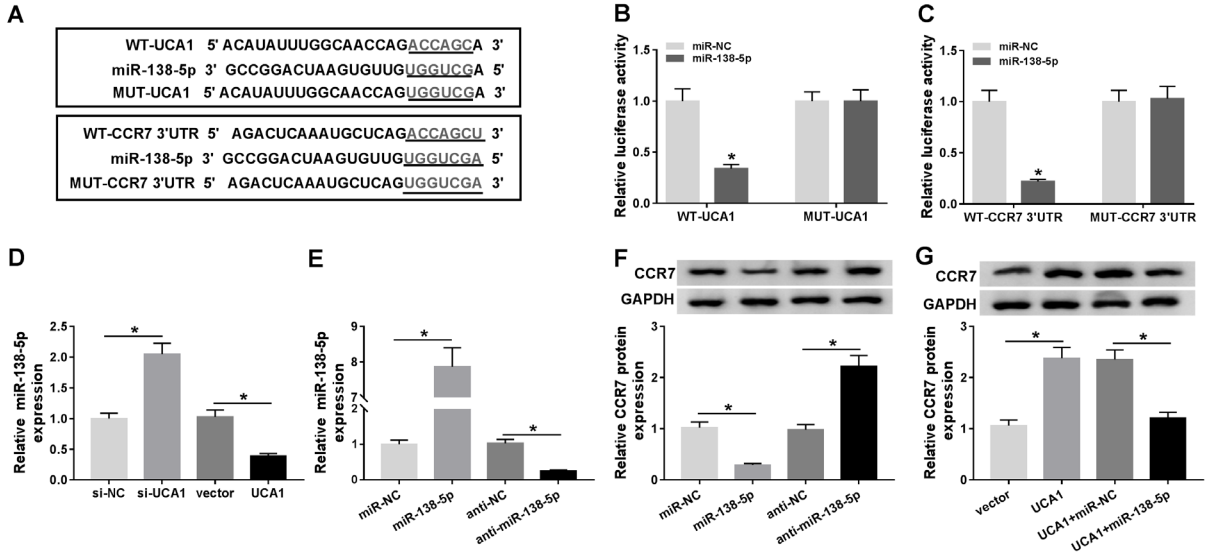

Figure 5. UCA1 regulated CCR7 expression through sponging miR-138-5p in CAL-27 cells. A) The sequences of UCA1 or CCR7 3'UTR containing the miR-138-5p binding sites or mutant binding sites were shown. B, C) Dual-luciferase reporter assay was used to detect the interaction between miR-138-5p and UCA1 or CCR7 in CAL-27 cells. D) qRT-PCR was performed to assess the expression of miR-138-5p in CAL-27 cells to measure the effect of UCA1 expression on miR-138-5p expression. E) The expression of miR-138-5p was determined by qRT-PCR to evaluate the transfection efficiency of miR-138-5p mimic and inhibitor. F) WB analysis was used to assess the protein level of CCR7 to detect the effect of the miR-138-5p expression on CCR7 expression. G) The protein level of CCR7 was measured by WB analysis to evaluate the overexpression of UCA1 and miR-138-5p on CCR7 expression. *p<0.05

by UCA1 and miR-138-5p (Figure 5G). Additionally, these results were also confirmed in UM1 cells (Supplementary Figure S4). Therefore, we concluded that UCA1 promoted CCR7 expression through sponging miR-138-5p.

miR-138-5p overexpression reversed the promotion effect of UCA1 overexpression on the progression of CAL-27 cells. To further confirm our results, we co-transfected UCA1 overexpression plasmid and miR-138-5p mimic into CAL-27 cells. As shown in Figure 6A, miR-138-5p mimic could reverse the inhibition effect of UCA1 overexpression on miR-138-5p expression, indicating that both transfections were successful. By measuring the number of cloned CAL-27 cells and the protein levels of c-myc, PCNA, and Ki-67, we uncovered that miR-138-5p overexpression could invert the promotion effect of overexpressed UCA1 on the proliferation of CAL-27 cells (Figures 6B, 6C). Further, the increasing effect of UCA1 overexpression on the migration and invasion of CAL-27 cells also could be reversed by miR-138-5p mimic, as demonstrated by the detection of the number of migrated and invaded CAL-27 cells and the protein levels of MMP2, MMP9, E-cadherin, and Vimentin (Figures 6D–6F). In addition, the promotion effect of UCA1 overexpression on the ECAR level, ATP level, glucose uptake, and lactate production of CAL-27 cells also could be recovered by miR-138-5p overexpression (Figures 6G–6J). More importantly, the same results were also confirmed in UM1 cells (Supplementary Figure S5). Hence, our results revealed that miR-138-5p was involved in the regulation of UCA1 on TSCC progression.

Interference of UCA1 reduced TSCC tumor growth *in vivo*. To further investigate the role of UCA1 in TSCC, we performed *in vivo* experiments. Through measurement of 28 d, we found that the tumor volume was significantly inhibited in the UCA1 knockdown group compared with the sh-NC group (Figure 7A). Moreover, we also discovered that the tumor weight of the sh-UCA1 group was markedly decreased (Figure 7B). Besides, we performed qRT-PCR to determine the effectiveness of sh-UCA1 and the results confirmed that UCA1 expression was remarkably suppressed in the sh-UCA1 group (Figure 7C). Furthermore, we also detected the expression of miR-138-5p and CCR7 in mice tumors using qRT-PCR and WB analysis, respectively. And

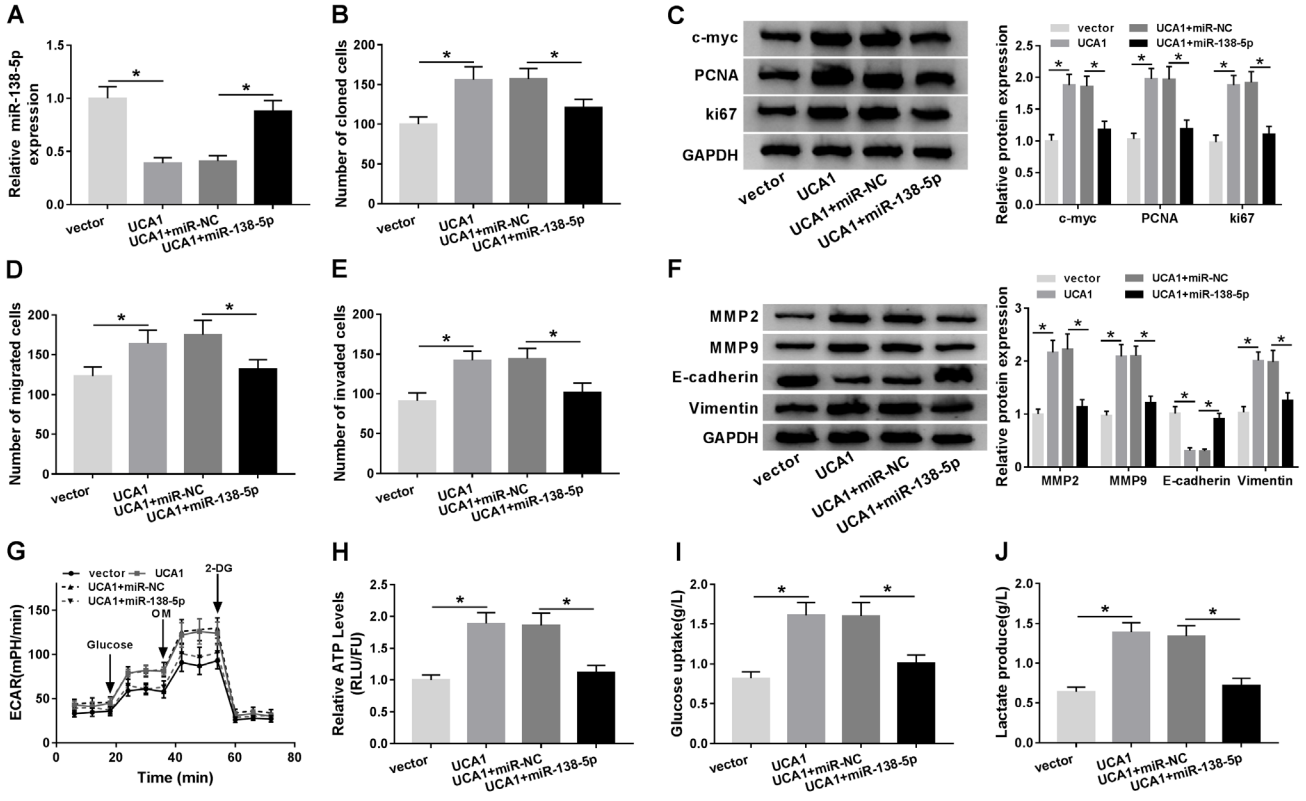

Figure 6. Effects of UCA1 overexpression and miR-138-5p overexpression on the progression of CAL-27 cells. CAL-27 cells were co-transfected with UCA1 overexpression plasmid and miR-138-5p mimic as described. A) The expression of miR-138-5p was tested by qRT-PCR to confirm the transfection efficiency of UCA1 overexpression plasmid and miR-138-5p mimic. B) The number of cloned CAL-27 cells was determined using colony formation assay. C) The protein levels of c-myc, PCNA, and Ki-67 in CAL-27 cells were measured by WB analysis. D, E) The number of migrated and invaded CAL-27 cells was examined by transwell assay. F) WB analysis was employed to assess the protein levels of MMP2, MMP9, E-cadherin, and Vimentin in CAL-27 cells. G) Seahorse XF Extracellular Flux Analyzer was performed to detect the ECAR of CAL-27 cells. H–J) The ATP, Glucose, and Lactate Assay Kits were used to evaluate the ATP level, glucose uptake, and lactate production of CAL-27 cells. *p<0.05

the results showed that the expression of miR-138-5p was remarkably enhanced, while CCR7 expression was obviously reduced in the sh-UCA1 group (Figures 7D, 7E). Hence, our results concluded that high UCA1 expression could increase CCR7 expression to promote the progression of TSCC by targeting miR-138-5p (Figure 7F).

Discussion

The development of TSCC cannot be separated from the interaction of various regulatory factors, including lncRNAs. Studies have shown that many lncRNAs are abnormally expressed in precancerous lesions of the oral cavity, which may be related to the progression of oral cancer [21]. Therefore, the study of lncRNAs is of great clinical value in TSCC. Here, we selected a lncRNA, UCA1, which was reported to be significantly upregulated in TSCC [14, 22]. Similar to previous studies, we also found that UCA1 was highly expressed in TSCC. Further experiments showed that the knockdown of UCA1 suppressed proliferation, migration, invasion, and glycolysis of TSCC cells, while the overexpression of it had the opposite effect. Also, silenced UCA1 reduced tumor growth of TSCC *in vivo*. These all indicated that UCA1 played a positive role in the development of TSCC.

The role of CCR7 in tumor metastasis has been demonstrated in many cancers [23, 24]. Wang et al. reported that CCR7 could also be involved in the proliferation of head and neck squamous cell carcinoma [25]. Besides, Liu et al. showed that CCR7 could promote dendritic cell migration by increasing glycolysis, and there was a negative feedback regulation [26]. A study by Guak et al. had shown that glycolytic metabolism was essential for CCR7 oligomerization [27]. This evidence indicated that CCR7 was not only related to proliferation and migration but also to glycolysis of cells. In our study, CCR7 was elevated in TSCC tissues and cells, which was consistent with the previous studies [19]. CCR7 expression was positively correlated with UCA1, and its expression was regulated by UCA1 *in vitro* and *in vivo*. The silencing of CCR7 inhibited proliferation, metastasis, and glycolysis of TSCC cells, and could reverse the promotion effect of UCA1 overexpression on TSCC progression. These results confirmed the key role of CCR7 in the proliferation, metastasis, and glycolysis of TSCC, and laid a foundation for the study of CCR7 in other diseases.

Many functions of lncRNAs in cancer have been clarified and are considered to play a key role in the development of cancers. We found that miR-138-5p had binding sites with UCA1 or CCR7. It has been reported that miR-138-5p suppressed cancer progression, including breast cancer, lung adenocarcinoma, and renal carcinoma [28–30]. Jiang et al. evidenced that miR-138 was downregulated in TSCC and participated in the proliferation and invasion of TSCC [31]. And Ji et al. indicated that AKT1, a target gene of miR-138, could regulate the migration and invasion abilities of TSCC [32]. Therefore, miR-138-5p might be a vital regulator of TSCC. Here, we confirmed that miR-138-5p expression was regulated by UCA1 *in vitro* and *in vivo*. Also, CCR7 expression was regulated by miR-138-5p and UCA1. Additionally, the reversal effect of miR-138-5p overexpression on UCA1 overexpression also once again confirmed that miR-138-5p participated in the regulation of UCA1 on the progression of TSCC. The discovery of miR-138-5p perfected the mechanism of UCA1, built a new bridge between UCA1 and CCR7, and provided a complete network for the clinical study of TSCC.

At present, it has been found that many lncRNAs can be used as markers of TSCC. For example, lncRNA CILA1 could serve as a biomarker for the chemosensitivity of TSCC tumors [33] and LINC00152 could function as a biomarker for the early detection and prognosis prediction of TSCC [34]. Therefore, continuous exploration of lncRNA function might provide a more theoretical basis for TSCC treatment. This study clarified the role of UCA1 in the progression of

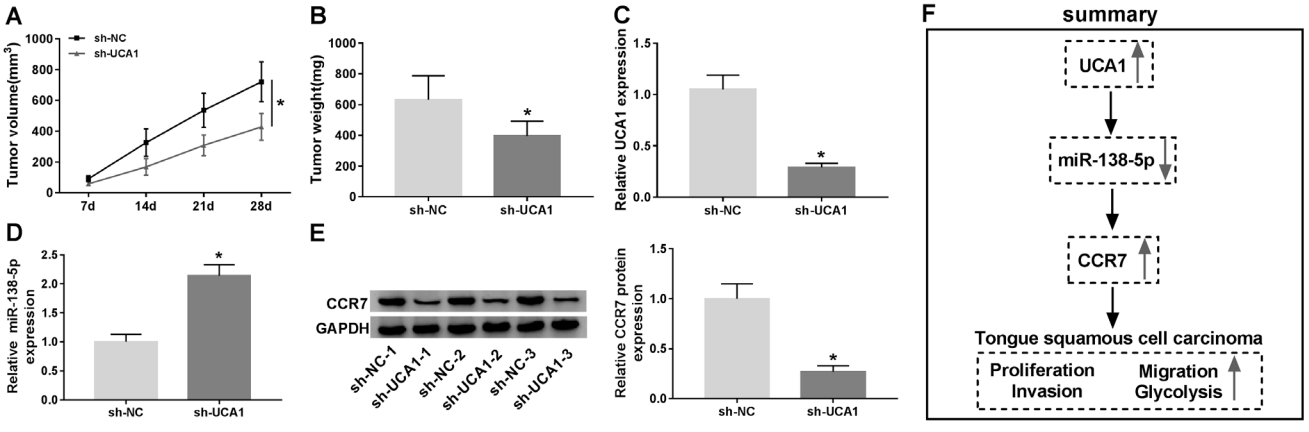

Figure 7. Effect of UCA1 interference on TSCC tumor growth *in vivo*. A) Tumor volume was calculated with length × width²/2 method at the indicated time points. B) Tumor weight was measured in mice. C, D) The expression of UCA1 and miR-138-5p in mice tumors were detected by qRT-PCR. E) WB analysis was performed to measure the protein level of CCR7 in mice tumors. F) The summary diagram of this study is shown. *p<0.05

TSCC and its potential molecular mechanism, which was of great clinical value for the treatment of TSCC.

In summary, we concluded that UCA1 played an oncogenic role in TSCC through regulating the miR-138-5p/CCR7 axis, which provided a reliable biomarker for the clinical treatment of TSCC.

Supplementary information is available in the online version of the paper.

References

[1] KIMPLE AJ, WELCH CM, ZEVALLOS JP, PATEL SN. Oral cavity squamous cell carcinoma--an overview. Oral Health Dent Manag 2014; 13: 877–882.

[2] LI Y, ZHAO Z, LIU X, JU J, CHAI J et al. Nomograms to estimate long-term overall survival and tongue cancer-specific survival of patients with tongue squamous cell carcinoma. Cancer Med 2017; 6: 1002–1013. https://doi.org/10.1002/cam4.1021

[3] MICHIKAWA C, UZAWA N, KAYAMORI K, SONODA I, OHYAMA Y et al. Clinical significance of lymphatic and blood vessel invasion in oral tongue squamous cell carcinomas. Oral Oncol 2012; 48: 320–324. https://doi.org/10.1016/j.oraloncology.2011.11.014

[4] ANNERTZ K, ANDERSON H, PALMER K, WENNERBERG J. The increase in incidence of cancer of the tongue in the Nordic countries continues into the twenty-first century. Acta Otolaryngol 2012; 132: 552–557. https://doi.org/10.3109/00016489.2011.649146

[5] KWOK ZH, TAY Y. Long noncoding RNAs: lincs between human health and disease. Biochem Soc Trans 2017; 45: 805–812. https://doi.org/10.1042/BST20160376

[6] DISTEFANO JK. The Emerging Role of Long Noncoding RNAs in Human Disease. Methods Mol Biol 2018; 1706: 91–110. https://doi.org/10.1007/978-1-4939-7471-9_6

[7] LI CH, CHEN Y. Targeting long non-coding RNAs in cancers: progress and prospects. Int J Biochem Cell Biol 2013; 45: 1895–1910. https://doi.org/10.1016/j.biocel.2013.05.030

[8] WU X, MA J, CHEN J, HUANG H. LncRNA CACS15 regulates tongue squamous cell carcinoma cell behaviors and predicts survival. BMC Oral Health 2019; 19: 231. https://doi.org/10.1186/s12903-019-0924-0

[9] JIA B, XIE T, QIU X, SUN X, CHEN J et al. Long noncoding RNA FALEC inhibits proliferation and metastasis of tongue squamous cell carcinoma by epigenetically silencing ECM1 through EZH2. Aging (Albany NY) 2019; 11: 4990–5007. https://doi.org/10.18632/aging.102094

[10] YANG H, FU G, LIU F, HU C, LIN J et al. LncRNA THOR promotes tongue squamous cell carcinomas by stabilizing IGF2BP1 downstream targets. Biochimie 2019; 165: 9–18. https://doi.org/10.1016/j.biochi.2019.06.012

[11] WANG XS, ZHANG Z, WANG HC, CAI JL, XU QW et al. Rapid identification of UCA1 as a very sensitive and specific unique marker for human bladder carcinoma. Clin Cancer Res 2006; 12: 4851–4858. https://doi.org/10.1158/1078-0432.CCR-06-0134

[12] YAO F, WANG Q, WU Q. The prognostic value and mechanisms of lncRNA UCA1 in human cancer. Cancer Manag Res 2019; 11: 7685–7696. https://doi.org/10.2147/CMAR.S200436

[13] GHAFOURI-FARD S, TAHERI M. UCA1 long non-coding RNA: An update on its roles in malignant behavior of cancers. Biomed Pharmacother 2019; 120: 109459. https://doi.org/10.1016/j.biopha.2019.109459

[14] FANG Z, WU L, WANG L, YANG Y, MENG Y et al. Increased expression of the long non-coding RNA UCA1 in tongue squamous cell carcinomas: a possible correlation with cancer metastasis. Oral Surg Oral Med Oral Pathol Oral Radiol 2014; 117: 89–95. https://doi.org/10.1016/j.oooo.2013.09.007

[15] BEN-BARUCH A. Organ selectivity in metastasis: regulation by chemokines and their receptors. Clin Exp Metastasis 2008; 25: 345–356. https://doi.org/10.1007/s10585-007-9097-3

[16] XU B, ZHOU M, QIU W, YE J, FENG Q. CCR7 mediates human breast cancer cell invasion, migration by inducing epithelial-mesenchymal transition and suppressing apoptosis through AKT pathway. Cancer Med 2017; 6: 1062–1071. https://doi.org/10.1002/cam4.1039

[17] ZHOU M, WANG S, HU L, LIU F, ZHANG Q et al. miR-199a-5p suppresses human bladder cancer cell metastasis by targeting CCR7. BMC Urol 2016; 16: 64. https://doi.org/10.1186/s12894-016-0181-3

[18] DU P, LIU Y, REN H, ZHAO J, ZHANG X et al. Expression of chemokine receptor CCR7 is a negative prognostic factor for patients with gastric cancer: a meta-analysis. Gastric Cancer 2017; 20: 235–245. https://doi.org/10.1007/s10120-016-0602-8

[19] FENG C, SO HI, YIN S, SU X, XU Q et al. MicroRNA-532-3p Suppresses Malignant Behaviors of Tongue Squamous Cell Carcinoma via Regulating CCR7. Front Pharmacol 2019; 10: 940. https://doi.org/10.3389/fphar.2019.00940

[20] SALMENA L, POLISENO L, TAY Y, KATS L, PANDOLFI PP. A ceRNA hypothesis: the Rosetta Stone of a hidden RNA language? Cell 2011; 146: 353–358. https://doi.org/10.1016/j.cell.2011.07.014

[21] GIBB EA, ENFIELD KS, STEWART GL, LONERGAN KM, CHARI R et al. Long non-coding RNAs are expressed in oral mucosa and altered in oral premalignant lesions. Oral Oncol 2011; 47: 1055–1061. https://doi.org/10.1016/j.oraloncology.2011.07.008

[22] WANG J, LI L, WU K, GE W, ZHANG Z et al. Knockdown of long noncoding RNA urothelial cancer-associated 1 enhances cisplatin chemosensitivity in tongue squamous cell carcinoma cells. Pharmazie 2016; 71: 598–602. https://doi.org/10.1691/ph.2016.6625

[23] WU J, LI L, LIU J, WANG Y, WANG Z et al. CC chemokine receptor 7 promotes triple-negative breast cancer growth and metastasis. Acta Biochim Biophys Sin (Shanghai) 2018; 50: 835–842. https://doi.org/10.1093/abbs/gmy077

[24] LI X, SUN S, LI N, GAO J, YU J et al. High Expression of CCR7 Predicts Lymph Node Metastasis and Good Prognosis in Triple Negative Breast Cancer. Cell Physiol Biochem 2017; 43: 531–539. https://doi.org/10.1159/000480526

[25] WANG S, JIN S, LIU MD, PANG P, WU H et al. Hsa-let-7e-5p Inhibits the Proliferation and Metastasis of Head and Neck Squamous Cell Carcinoma Cells by Targeting Chemokine Receptor 7. J Cancer 2019; 10: 1941–1948. https://doi.org/10.7150/jca.29536

[26] LIU J, ZHANG X, CHEN K, CHENG Y, LIU S et al. CCR7 Chemokine Receptor-Inducible lnc-Dpf3 Restrains Dendritic Cell Migration by Inhibiting HIF-1alpha-Mediated Glycolysis. Immunity 2019; 50: 600–615 e615. https://doi.org/10.1016/j.immuni.2019.01.021

[27] GUAK H, AL HABYAN S, MA EH, ALDOSSARY H, AL-MASRI M et al. Glycolytic metabolism is essential for CCR7 oligomerization and dendritic cell migration. Nat Commun 2018; 9: 2463. https://doi.org/10.1038/s41467-018-04804-6

[28] ZHAO C, LING X, LI X, HOU X, ZHAO D. MicroRNA-138-5p inhibits cell migration, invasion and EMT in breast cancer by directly targeting RHBDD1. Breast Cancer 2019; 26: 817–825. https://doi.org/10.1007/s12282-019-00989-w

[29] ZHU D, GU L, LI Z, JIN W, LU Q et al. MiR-138-5p suppresses lung adenocarcinoma cell epithelial-mesenchymal transition, proliferation and metastasis by targeting ZEB2. Pathol Res Pract 2019; 215: 861–872. https://doi.org/10.1016/j.prp.2019.01.029

[30] XIONG Y, ZHANG J, SONG C. CircRNA ZNF609 functions as a competitive endogenous RNA to regulate FOXP4 expression by sponging miR-138-5p in renal carcinoma. J Cell Physiol 2019; 234: 10646–10654. https://doi.org/10.1002/jcp.27744

[31] JIANG L, DAI Y, LIU X, WANG C, WANG A et al. Identification and experimental validation of G protein alpha inhibiting activity polypeptide 2 (GNAI2) as a microRNA-138 target in tongue squamous cell carcinoma. Hum Genet 2011; 129: 189–197. https://doi.org/10.1007/s00439-010-0915-3

[32] JI M, WANG W, YAN W, CHEN D, DING X et al. Dysregulation of AKT1, a miR-138 target gene, is involved in the migration and invasion of tongue squamous cell carcinoma. J Oral Pathol Med 2017; 46: 731–737. https://doi.org/10.1111/jop.12551

[33] LIN Z, SUN L, XIE S, ZHANG S, FAN S et al. Chemotherapy-Induced Long Non-coding RNA 1 Promotes Metastasis and Chemo-Resistance of TSCC via the Wnt/beta-Catenin Signaling Pathway. Mol Ther 2018; 26: 1494–1508. https://doi.org/10.1016/j.ymthe.2018.04.002

[34] YU J, LIU Y, GUO C, ZHANG S, GONG Z et al. Upregulated long non-coding RNA LINC00152 expression is associated with progression and poor prognosis of tongue squamous cell carcinoma. J Cancer 2017; 8: 523–530. https://doi.org/10.7150/jca.17510

Long noncoding RNA UCA1 regulates CCR7 expression to promote tongue squamous cell carcinoma progression by sponging miR-138-5p

T. T. SHI, R. LI, L. ZHAO*

Supplementary Information

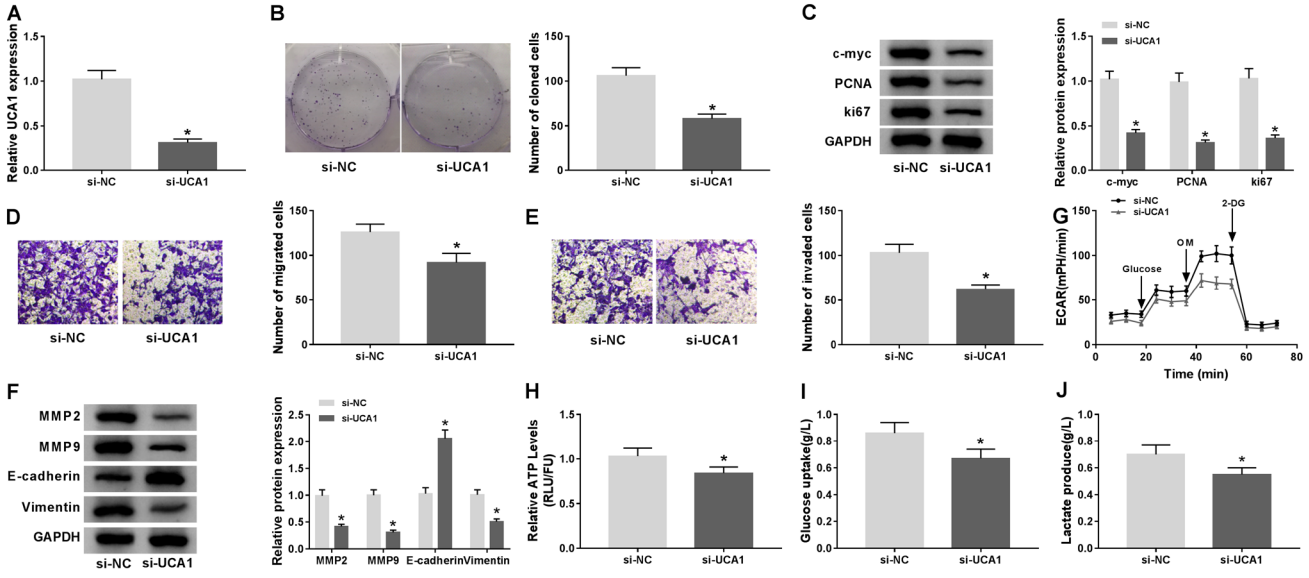

Supplementary Figure S1. Effect of UCA1 silencing on the progression of UM1 cells. UM1 cells were transfected with si-UCA1 or si-NC. A) UCA1 expression was detected by qRT-PCR to assess the transfection efficiency of si-UCA1. B) Colony formation assay results revealed that silenced UCA1 hindered the proliferation of UM1 cells. C) WB analysis results indicated that UCA1 silencing could suppress the protein levels of c-myc, PCNA, and Ki-67 in UM1 cells. D, E) Transwell assay results suggested that the migration and invasion of UM1 cells were restrained by UCA1 knockdown. F) WB analysis was used to detect the protein levels of MMP2, MMP9, E-cadherin, and Vimentin in UM1 cells. G) The ECAR of UM1 cells was measured by Seahorse XF Extracellular Flux Analyzer. H–J) The ATP level, glucose uptake, and lactate production of UM1 cells were inhibited by UCA1 silencing. *$p<0.05$

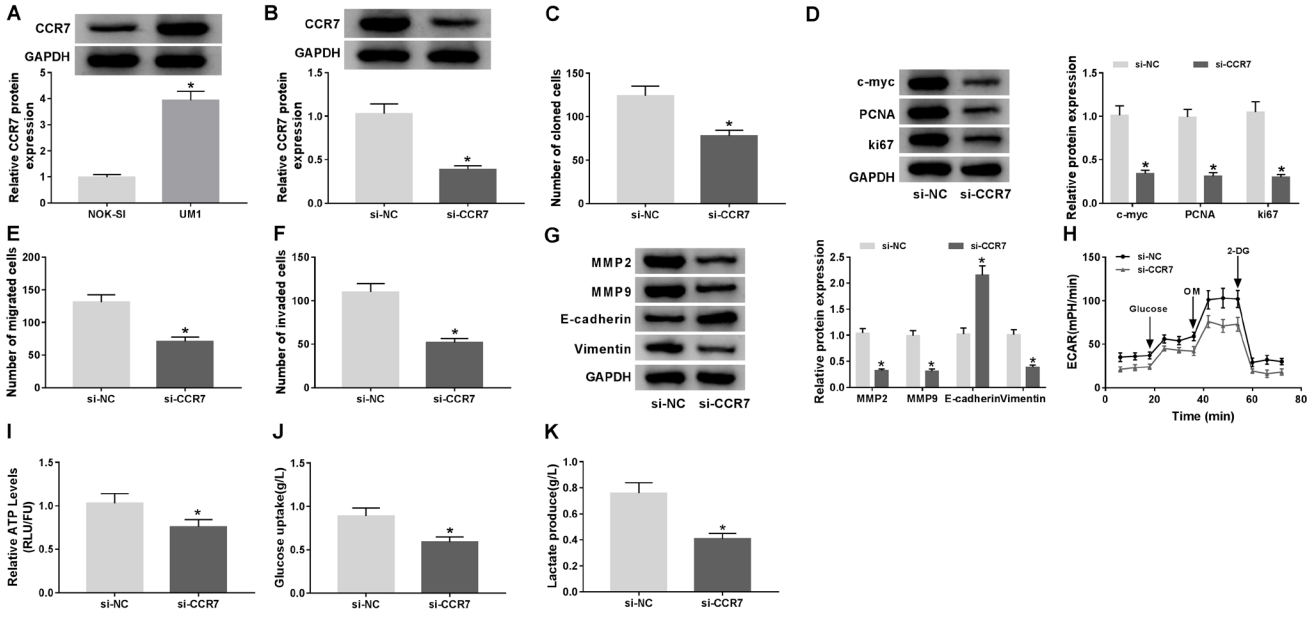

Supplementary Figure S2. Effect of CCR7 silencing on the progression of UM1 cells. A) WB analysis revealed that the protein level of CCR7 in UM1 cells was higher than that in NOK-SI cells. B–K) UM1 cells were transfected with si-CCR7 or si-NC. (B) The transfection efficiency of si-CCR7 was assessed by detection of the protein level of CCR7 using WB analysis. (C) Colony formation assay results indicated that CCR7 silencing could restrain the proliferation of UM1 cells. (D) WB analysis revealed that the protein levels of c-myc, PCNA, and Ki-67 in UM1 cells could be suppressed by CCR7 silencing. (E–F) Transwell assay results showed that silenced CCR7 could inhibit the migration and invasion of UM1 cells. (G) WB analysis was used to determine the protein levels of MMP2, MMP9, E-cadherin, and Vimentin in UM1 cells. (H) The ECAR of UM1 cells was measured by Seahorse XF Extracellular Flux Analyzer. (I–K) The ATP level, glucose uptake, and lactate production of UM1 cells were suppressed by CCR7 knockdown. *p<0.05

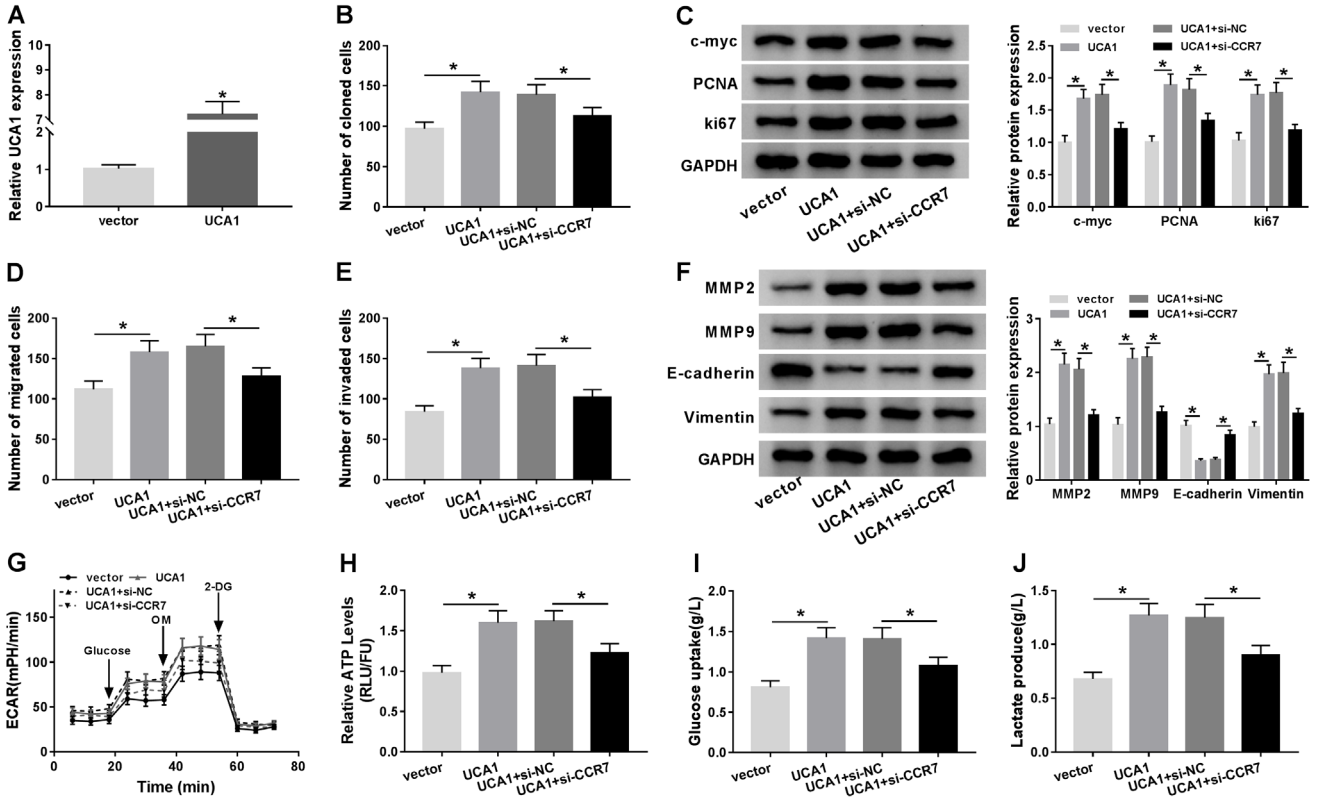

Supplementary Figure S3. Effects of UCA1 overexpression and CCR7 knockdown on the progression of UM1 cells. A) qRT-PCR was used to evaluate the transfection efficiency UCA1 overexpression plasmid. B–J) UM1 cells were co-transfected with UCA1 overexpression plasmid and si-CCR7. (B) Colony formation assay was performed to measure the number of cloned UM1 cells. (C) WB analysis was used to determine the protein levels of c-myc, PCNA, and Ki-67 in UM1 cells. (D–E) The number of migrated and invaded UM1 cells was detected by transwell assay. (F) The protein levels of MMP2, MMP9, E-cadherin, and Vimentin in UM1 cells were assessed by WB analysis. (G) Seahorse XF Extracellular Flux Analyzer was used to test the ECAR of UM1 cells. (H–J) The ATP level, glucose uptake, and lactate production of UM1 cells were determined by their corresponding Assay Kits. *p<0.05

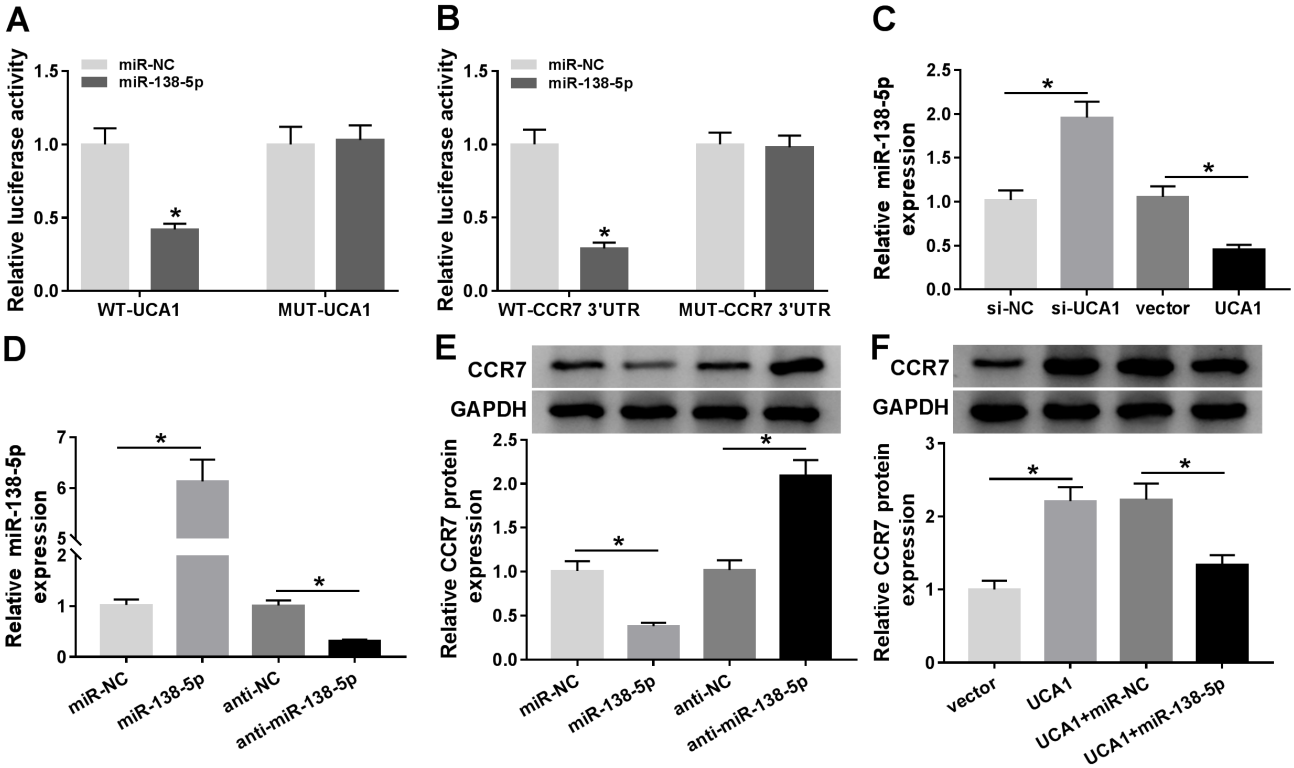

Supplementary Figure S4. UCA1 regulated CCR7 expression through sponging miR-138-5p in UM1 cells. A, B) Dual-luciferase reporter assay was used to detect the interaction between miR-138-5p and UCA1 or CCR7 in UM1 cells. C) qRT-PCR was performed to assess the expression of miR-138-5p in UM1 cells to measure the effect of UCA1 expression on miR-138-5p expression. D) The expression of miR-138-5p was determined by qRT-PCR to evaluate the transfection efficiency of miR-138-5p mimic and inhibitor in UM1 cells. E) WB analysis was used to assess the protein level of CCR7 to detect the effect of the miR-138-5p expression on CCR7 expression in UM1 cells. F) The protein level of CCR7 was measured by WB analysis to evaluate the overexpression of UCA1 and miR-138-5p on CCR7 expression in UM1 cells. *$p<0.05$

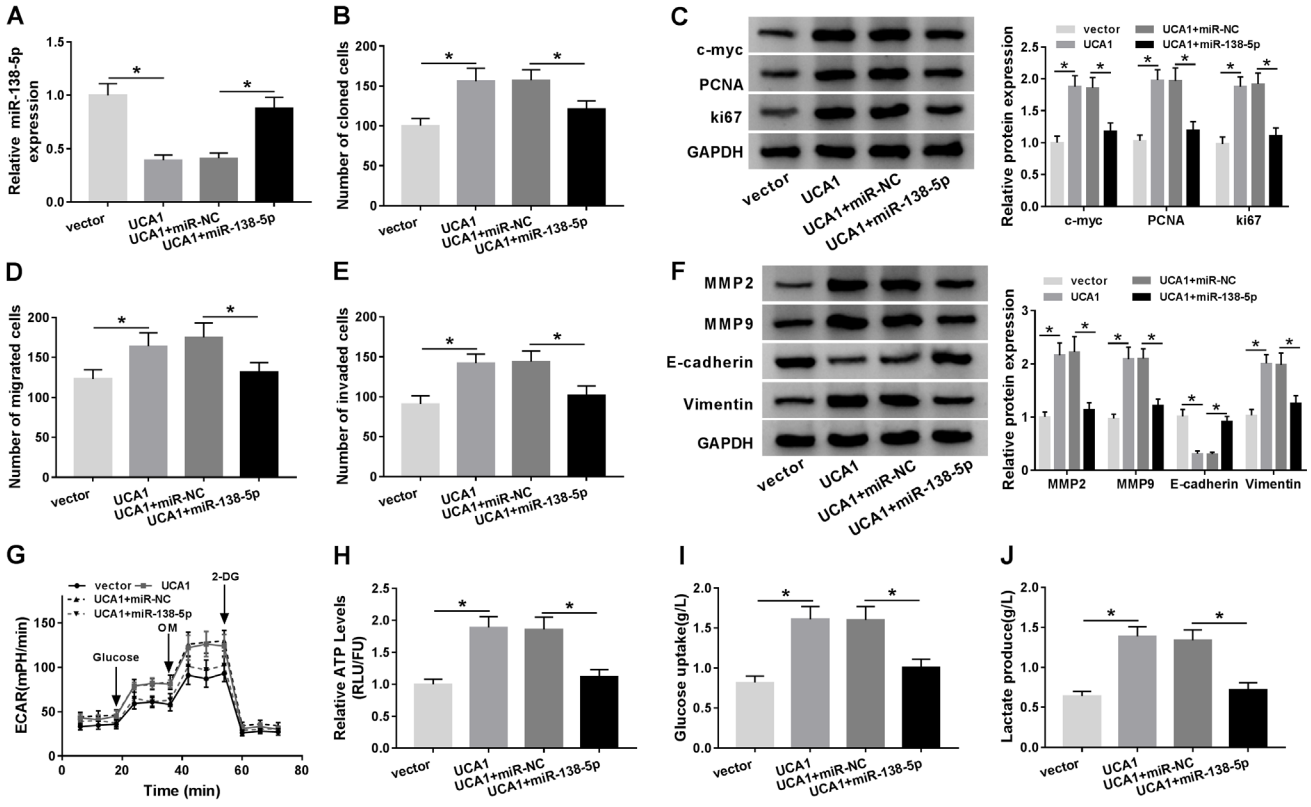

Supplementary Figure S5. Effects of UCA1 overexpression and miR-138-5p overexpression on the progression of UM1 cells. UM1 cells were co-transfected with UCA1 overexpression plasmid and miR-138-5p mimic. A) The expression of miR-138-5p was tested by qRT-PCR. B) The number of cloned UM1 cells was determined using colony formation assay. C) The protein levels of c-myc, PCNA, and Ki-67 in UM1 cells were measured by WB analysis. D, E) The number of migrated and invaded UM1 cells was examined by transwell assay. F) WB analysis was employed to assess the protein levels of MMP2, MMP9, E-cadherin, and Vimentin in UM1 cells. G) Seahorse XF Extracellular Flux Analyzer was performed to detect the ECAR of UM1 cells. H–J) The ATP, Glucose, and Lactate Assay Kits were used to examine the ATP level, glucose uptake, and lactate production of UM1 cells. *p<0.05